Excerpt from the Proceedings of the 2011 COMSOL Conference in Boston

Modeling System Dynamics in a MEMS-Based Stirling Cooler

Dongzhi Guo[1], Alan J. H. McGaughey[1], Gary K. Fedder[2], Minyoung Lee[1] and Shi-Chune Yao[*,1]
[1]Department of Mechanical Engineering, Carnegie Mellon University
[2]Department of Electrical & Computer Engineering, Carnegie Mellon University
*Corresponding author: SH-311, 5000 Forbes Avenue, Pittsburgh, PA 15213. Email: scyao@cmu.edu

Abstract: Micro-scale devices based on the Stirling cycle are an attractive choice for chip- and board-level electronics. A new Stirling cycle micro-refrigeration system composed of arrays of silicon MEMS cooling elements has been designed. COMSOL is used to evaluate the thermal performance of the system. Simulation of compressible flow and heat transfer with a large deformed mesh has been successfully implemented and is used to determine the cooling capacity and coefficient of performance, *COP*. Future work will focus on modeling the coupling of the thermal fluid phenomena with electrostatics.

Keywords: Stirling cooler, Arbitrary Lagrangian-Eulerian (ALE), *COP*

1. Introduction

Micro-scale coolers have wide potential application areas, such as cooling for chip- and board-level electronics, sensors and radio frequency systems [1]. Thermoelectric coolers are the most common refrigeration devices and have been scaled to the micro-domain. Significant challenges exist in the design and fabrication of thermoelectric materials that can achieve a high efficiency of thermoelectric energy conversion [2]. Micro-scale devices operating on the Stirling cycle are an attractive potential alternative due to the high efficiencies realized for macro-scale Stirling machines [3]. The development of MEMS technologies makes the miniaturization of Stirling systems possible. To our knowledge, the first attempt to approach the micro-scale is documented in a series of cryocooler patents [4-8]. Subsequent efforts on a prototype micro-scale Stirling cooler addressed frictional losses and leakage concerns by replacing conventional pistons and the associated linkages with electrostatically-driven diaphragms. No actual devices have been made.

A new micro-scale Stirling cooler system, which includes two diaphragm actuators and a regenerator that separates the hot and cold chambers, has been designed and the fabrication is underway. One element of the Stirling micro-cooler is shown conceptually in Fig. 1(a). The cooling element is initially designed to be 5 mm-long, 2.5 mm-wide, have a thickness of 150 μm, and is fabricated on a silicon wafer, as illustrated in Fig. 1(b). The design minimizes conduction heat losses across a 0.5 mm-long regenerator by distancing the compressor and expander assemblies with a low thermal conductivity passage housing a working fluid (e.g., air) pressurized at 2 bar. The compression and expansion sides are driven by 2.25 mm circular diaphragms electrostatically. In the regenerator, an array of vertical silicon pillars serves as a thermal capacitor transferring heat to and from the working gas during a cycle. Channels are opened in the silicon substrate between the chambers and the regenerator to allow the working fluid to pass through. Under operating conditions, the hot and cold diaphragms oscillate sinusoidally and 90° out of phase such that the heat is extracted to the cold chamber and released from the hot chamber.

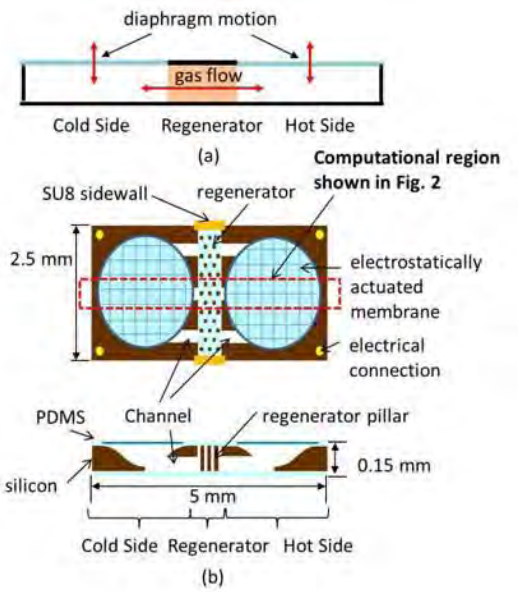

Figure 1. (a) Conceptual schematic of a single element of the Stirling micro-cooler. (b) Top: plan view; and Bottom: cross-sectional view of the element.

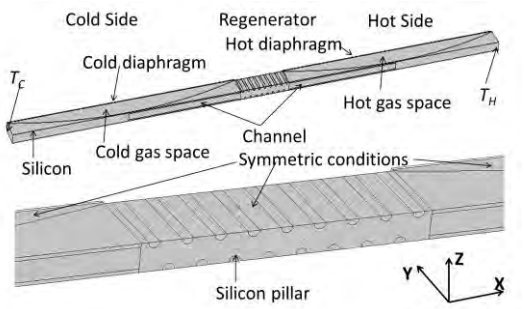

Figure 2. Computational region and boundary conditions.

Our interest is the cooling capacity provided by the Stirling cycle and the cooling efficiency. The compressible fluid and heat transfer models are used in COMSOL to evaluate the thermal performance.

2. Problem Description

One full element is shown in Fig.1. A key design feature is the regenerator between the hot and cold sides. Staggered circular silicon pillars with 20 μm diameter are used for heat storage. The volume fraction of the silicon in the regenerator is 0.11 and there are about 390 pillars. A full system model for our device is not realistic due to the number of the pillars, which makes the geometrical features very complex. In order to capture the flow characteristics across the pillars and the heat transfer effect of the regenerator accurately, a slice of the system element, shown in Fig. 2, is considered as the model object.

2.1 Governing Equations

For compressible laminar flow and heat transfer, the governing equations are the continuity equation,

$$\frac{\partial \rho}{\partial t} + \nabla \cdot (\rho \vec{u}) = 0, \qquad (1)$$

the momentum equation,

$$\rho \frac{\partial \vec{u}}{\partial t} + \rho(\vec{u} \cdot \nabla)\vec{u} = -\nabla \mathrm{p} - \nabla \cdot \bar{\bar{\tau}}, \qquad (2)$$

and the energy equation

$$\rho C_p \left[\frac{\partial T}{\partial t} + (\vec{u} \cdot \nabla)\mathrm{T}\right] = \nabla \cdot (k \nabla T) + \bar{\bar{\tau}} : \nabla \vec{u} - \frac{T}{\rho}\frac{\partial \rho}{\partial T}\left(\frac{\partial p}{\partial t} + \vec{u} \cdot \nabla p\right). \qquad (3)$$

Here, ρ is the fluid density, $\vec{u}$ is the velocity vector, p is the pressure, C_p is the gas specific heat capacity, T is the temperature, k is the thermal conductivity of the gas, and $\bar{\bar{\tau}}$ is the viscous tensor

$$\bar{\bar{\tau}} = \mu[\nabla \vec{u} + (\nabla \vec{u})^T] - \frac{2}{3}\mu(\nabla \cdot \vec{u}), \qquad (4)$$

where μ is the dynamic viscosity of the gas.

Assuming the gas in the system to be ideal, the state equation of the gas is

$$\rho = \frac{pM_g}{RT}, \qquad (5)$$

where R is the ideal gas constant and M_g is the molar mass of the gas.

In the solid part, the energy equation is

$$\rho_s C_{p_s} \frac{\partial T}{\partial t} = \nabla \cdot (k_s \nabla T), \qquad (6)$$

where ρ_s, C_{p_s} and k_s are the density, specific heat capacity, and thermal conductivity of the solid material.

2.1 COMSOL Setup and Boundary Conditions

COMSOL 4.2 was used for the 3D model simulation shown in Fig. 2. The main module used for solving the governing equations is the Non-isothermal Flow module. The ALE (Arbitrary Lagrangian-Eulerian) moving mesh method was used to handle the domains (cold and hot gas space shown in Fig. 2), where there are moving boundaries. The second geometry shape order and Winslow mesh smoothing method were used in Frame Settings. As the displacement of the diaphragm is large, this caused a large distortion of the mesh in the free domains (cold and hot gas space shown in Fig. 2). In order to solve this problem and make the calculation converge, the Solid Mechanics module, which describes the motion of the diaphragms, was added for the moving diaphragms.

The computational region and boundary conditions are shown in Fig. 2. The gas and solid parts are air and silicon. As the diaphragms are driven electrostatically, their actual motions are very complicated and require further study. To simplify the model and the analysis, a sinusoidal motion with a 90° phase lag is applied for the cold and hot diaphragms. The displacement of

the cold diaphragm is

$$y(x,t) = Y_{max}(x)\sin(2\pi ft); \quad (7)$$

The displacement of the hot diaphragm is $y(x,t) = Y_{max}(x)\sin(2\pi ft - \pi/2)$, for $t \geq \frac{1}{4f}$. (8)

f is the operating frequency, which is 100 Hz, and $Y_{max}(x)$ is the vibration amplitude of the diaphragm at different x positions. A 5 μm gas gap is left above the silicon substrate to avoid the contact between the silicon and the diaphragm when the diaphragm moves to the bottom position. The no slip condition is applied to the gas-solid interface. The initial pressure in the system is 2 bar. The left surface temperature is constant and is T_C= 288.15 K. The right surface has a constant temperature of T_H= 313.15 K. The remaining surfaces are thermally insulated. The initial temperature for the whole region is 293.15 K. The mesh structure is tetrahedral. The mesh number is 369,766 and the number of degrees of freedom is 735,167.

3. Result and Discussion

Steady state is reached after 15 cycles. At steady state, the temperature contour results at t=0.2425 s and t=0.2475 s in one cycle are shown in Figs. 3 and 4. In Fig. 3, the cold diaphragm is compressed totally and the hot gas space has a highest temperature at this moment of the cycle. In Fig. 4, when the hot diaphragm is flat and the cold gas space is expanded totally. At this time, the cold gas space has a lowest temperature. So the heat is transferred to the cold side and the heat is released in the hot side, as we require.

The time dependence of the space-averaged hot-side and cold-side temperatures is shown in Fig. 5. In the cold gas space, the space-averaged temperature oscillates between 260 K and 291 K, and the hot side space-averaged temperature oscillates between 312 K and 344 K. The time- and space-averaged temperature in the cold and hot space are277.5 K, which is 10.65 K below T_C, and 322.5 K, which is 9.35 K above T_H.

The space-averaged heat flux coming into the cold side from the left surface of the system, which has a constant temperature T_C, is shown in Fig. 6. The heat flux Q is the cooling capacity of the Stirling cooler element. From this figure, we can obtain an average cooling capacity of 3.74

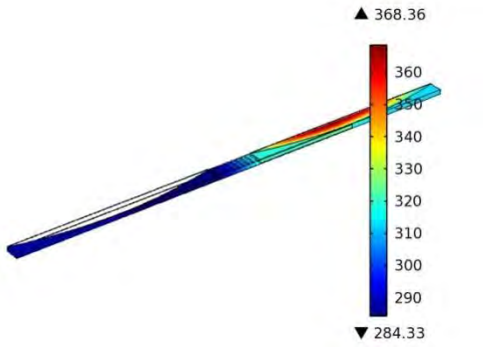

Figure 3. Temperature contour of the system at t=0.2425 s.

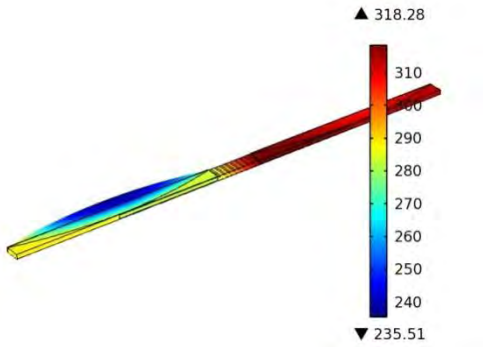

Figure 4. Temperature contour of the system at t= 0.2475 s.

W/cm^2. The corresponding heat flow rate q is 0.00027 W.

The coefficient of performance (COP) of a cooleris the ratio of the heat removal, q, to the input work, W,

$$COP = \frac{q}{W}. \quad (9)$$

Fig. 7 gives the P-V cycle of the system during steady state operation. The pressure is the space-averaged pressure of all the gas space regions, and the volume is the total gas volume. The work per cycle is the area covered by the P-V curve, which is 4.85 E (-7) J. The frequency is 100 Hz, so the work input W is 4.85 E (-5) W. According to Eq. (9), COP of the system is 5.6. The Carnot coefficient of performance COP_C, which represents the maximum theoretical efficiency possible between constant temperature hot and cold sources, can be found from $COP_C = \frac{T_C}{T_H - T_C}$. For T_H =313.15 K and T_C =288.15 K, COP_C is 11.5. The percent of Carnot figure of merit provides a gauge of how closely a proposed cycle or device is approaching the theoretical limit. The ratio of the actual coefficient of

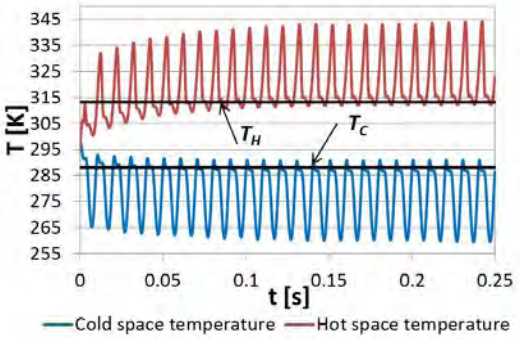

Figure 5. Space-averaged temperature as a function of time.

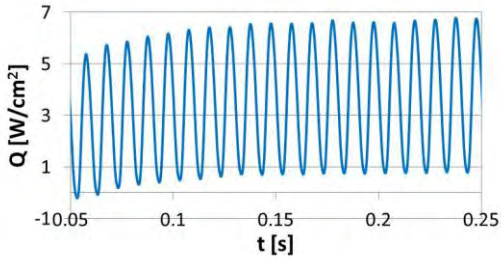

Figure 6. Averaged heat flux coming into the cold side.

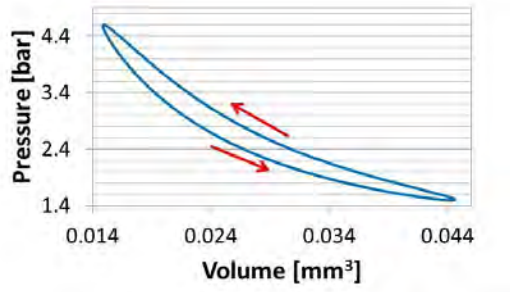

Figure 7. *P-V* cycle of the system during steady state operation.

performance to that of the Carnot cycle is $\frac{COP}{COP_C} =$ 48.7%.

4. Conclusions and Future Work

The COMSOL Mutiphysics program has been used to simulate of a new Stirling micro-scale cooler. The model results predict the cooling capacity and *COP* of the system. More work will be done to obtain the performance of the whole device. The regenarator and the dead space will be replaced by porous media module for simplifying the full system model. In addition, as the diaphragms are driven by electrostatic forces, the system model coupling with electrostatics is to be studied for obtaining a more accurate motion of the diaphragms.

5. References

1.Moran, M.E., et al., Microsystem Cooler Development, *2nd International Energy Conversion Engineering Conference (IECEC)*, Providence, RI, Aug 16-19(2004).

2. Sharp, J., Bierschenk, J. and Lyon, H.B., Overview of Solid-state Thermoelectric Refrigerators and Possible Applications to On chip Thermal Management,*Proc. IEEE*, v.94, no.8, pp.1602-1612(2006).

3. Burger, J.F.,CryogenicMicrocooling, PhD Thesis, University of Twente, Netherlands, 2001.

4. Stetson, N.B., Miniature Integral Stirling Cryocooler, *U.S. Patent* No. 5,056,317, October 15, 1991.

5. Solomon, R., Integrated Refrigerated Computer Module, *U.S. Patent* No. 5,349,823 (Assignee: Intel Corp.), September 27, 1994.

6. Bowman, L., et al., MicrominiatureStirling Cycle Cryocoolers and Engines, *U.S. Patent* No. 5457956 and continued-in-part in 5749226 and 5941079.

7. Moran, M.E., et al., Micro-Scale Regenerative Heat Exchanger, *AIAA Canada-Europe-USA-Asia (CANEUS) 2004 Conference on Micro-Nano-Technologies for Aerospace Applications*, Monterey, CA, Nov. 1-5, 2004.

8. Moran, M.E., Micro-Scalable Thermal Control Device, *US Patent* No. 6,385,973 B1, May 14, 2002.

6. Acknowledgements

This work was supported by the Defense Advanced Research Projects Agency (DARPA) under Grant No. W31P4Q-10-1-0015.